STUDIES ON STRUCTURAL AND OPTICAL PROPERTIES OF $LiFePO_4$ THIN FILMS

T. BALAKRISHNAN[a*], N. SANKARASUBRAMANIAN[a],
A. KATHALINGAM[b]
[a]*Thin FilmResearchLaboratory, Department of Physics, Thiagarajar college of Engineering, Madurai – 625 015, Tamil Nadu State, India*
[b]*Millimeter-wave Innovation Technology (MINT) Research Center, Dongguk University, Seoul-04620, South Korea*

$LiFePO_4$ thin films were synthesized using cost effective spin coating method coupled with sol-gel process.Theprepared $LiFePO_4$ thin films were characterized by X-ray diffraction (XRD), UV-visible spectroscopy, Fourier Infrared Spectroscopy and Scanning Electron Spectroscopy. Grain size of the film was found to increase with the number of coating cycles. The films showed high optical transmittance over 90.75% in the visible range. Optical band gap energy of the films evaluated from optical absorption data was about 3.4 eV.Thickness and grain size of the films are increased with the number of spin coating cycles. Crystallization is increased at higher coating cycles. The band gap values are found to vary between 3.4 eV and 3 eV depending upon number of coating cycles.

(Received February 12, 2017; Accepted July 11, 2017)

Keywords: $LiFePO_4$, Thin film, Sol-gel process,Spin coating, Li-ion battery

1. Introduction

Secondary lithium-ion (Li-ion) batteries are used in a wide range of applications due to their high capacity, high electrochemical potential, superior energy density, durability and high flexibility in design. These outstanding properties of Li-ion batteries accelerate the substitution of conventional secondary batteries. There is an increasing demand of Li-ion batteries due to their low cost, safe and environmentally compatible positive electrodes [1-5]. Amongst the cathode materials available iron-based LiFePO4 is attractive due to high theoretical specific capacity ~170 mAh g^{-1}, high power capability, good cycleability, non-toxicity and safety. [H. Mazor, D. Golodnitsky, L. Burstein, A. Gladkich, E. Peled, Electrophoretic deposition of lithium iron phosphate cathode for thin-film 3D-microbatteries, Journal of Power Sources 198 (2012) 264–272]. Moreover, the use of iron based compounds in battery materials is quite attractive as the Fe is abundant, inexpensive and low toxic compared to Co, Ni and Mn.

Hence, lithium iron phosphate ($LiFePO_4$), an ordered Olivine type compound is under extensive studies as one of the most promising cathode material. It has more favored properties such as low cost, environmental compatibility, less toxicity, high thermal stability and high specific capacity compared to the $LiCoO_2$and $LiMn_2O_4$.Most exciting advantageof $LiFePO_4$is its stability with high voltage application, hardly changes while Li-ion intercalation and de-intercalation.In Li-ion battery lithium ions are extracted from anode to cathode during discharge process and it is reversed during charging. During electrochemical process, $FePO_4$ is present as second phase.

The extraction and insertion of lithium ion during charging and recharging process may be written as Equ. (1) and Equ. (2), respectively [6-8].

$$LiFePO_4 - xLi^+ - xe^- \longrightarrow FePO^4 + (1-x)LiFePO^4 \quad (1)$$

$$FePO^4 + xLi^+ + xe^- \longrightarrow LiFePO^4 + (1-x)FePO^4 \quad (2)$$

Several groups have recently reported deposition of $LiFePO_4$ thin film using Electrostatic spray deposition [9,10], Dip Coating [11], Ion beam sputtering [12], RF Magnetron sputtering [13,14], Ionized magnetron sputtering [15], Pulsed laser deposition [16-19], Chemical vapor deposition [20], Ultra short laser radiation [21], Electro spinning method [22], Screen printing process [23], Ink-Jet printing [24], Electrochemical method [25], Aerosol deposition [26] and Spin coating Technique [27]. $LiFePO_4$thin films prepared by various methods differ much from their properties, which is mainly due to synthesis induced changes on $LiFePO_4$ properties.

Sol gel spin coating method is an alternative procedure for the deposition of $LiFePO_4$thin film cathodes owing to its simple, excellent control of stoichiometry, and easy control of crystallinity, density and micro structure. It has been well demonstrated that the sol-gel process offers good mixture of the starting materials. However, quality of the deposited thin films is highly dependent on the nature of precursor solution, chemical stability and adherence to substrate surface. Smooth and highly adherent films can be prepared in sol gel process using highly homogeneous solution. The major objective of this study was to prepare crack- free smooth $LiFePO_4$ thin films by simple and efficient sol gel technique and study their optical, electrical and structural properties.

2. Experimental

Spin coating solution was prepared by dissolving Lithium phosphate monobasic (LiH_2PO_4) and iron (III) nitrate nonahydrate (Fe $(NO_3)3.9H_2O$) in deionized water with an element ratio Li:Fe:P = 1:1:1. Toobtain homogeneoussolution,wasstirred using magnetic stirrer for 1 hour at ambient temperature. Mixed solution was then transferred to reflux unit at 60 ^{0}C for about an hour to remove the water. The resultant gel was washed with methanol (CH_3OH) then transferred to reflux unit at 50 ^{0}C and this process was repeated two times. Finally, desired concentration solution was obtained adding with methanol, air cooled and then allowed for ageing.

The glass substrates were cleaned using double distilled water, then concentrated chromic acid. After thatthey were ultrasonicallycleaned with acetone,finallydried.

The prepared solution was spun onto substrates at 3500 rpm for 10 s using a spin coater, then it was heated treated at 375^{o}C using a furnace for 5 min to evaporate solvents and organic materials from the solutes. The above process was repeated for 8-12 times to get final as-deposited films.Before the characterization prepared thin films were subjected to thermal annealing in an argon atmospherefor 1h at 700^{o}C. The chemical reaction executed to form the final product is as follows:

$$LiH_2PO_4 + Fe(NO_3)_3 + 2H_2 = LiFePO_4 + 3NO_2 \uparrow + 3H_2O \uparrow \quad (3)$$

Powder X-ray diffraction (XRD) studies were carried out using Philips Pan-analytical diffractometer withCuKα radiations to measure the crystallinity, phase, micro strain, dislocation density, lattice parameter, texture coefficient and standard deviation values to assess the conditions of the prepared films. Surface Morphology features were examined using Scanning Electron Microscope (SEM). Fourier-Transform Infrared (FT-IR) spectroscopy analysis was carried out using Shimadzu spectrophotometer to study the configuration of molecular spices and changes in the coordination of the compound. UV-Vis absorption spectra were recorded using UV -3101 Shimazdu visible spectrophotometer. Electrical characterization of thin film was carried out using four probe techniques.

3. Results and Discussion

3.1. Rheological Properties of Lithium Iron Phosphate Sol Solution

Rheological properties of prepared lithium iron phosphate Sol solution have been investigated by measuring its density and viscosity for a particular time duration. The prepared solution became increasingly cloudy when allowed for aging at room temperature. Density of the

solution was measured periodically using ostwald viscometer. It has been observed that viscosity increased slowly during the initial period of aging then subsequently a sudden rise in viscosity was observed at a stage called break off point and reached a steady state at a stage called saturation point. The increase in the viscosity was due to the occurrence of polymerization, i.e., condensation. This saturation behavior indicates the colloidal nature of gelatinous suspension. Thus, by following microscopic changes of solution during the aging period, the break off and saturation point were noted to determine the critical time $t_{1/2}$ and a graph was plotted between observed values of viscosity and the number of days during aging.

This process was carried out for different concentrations of precursor solutions and the results are presented in Fig 1. Critical time period is the suitable and ideal time to coat the films, which can result in significant properties. The critical time $t_{1/2}$ of the prepared solution was found to be 3rd day of aging period. Hence, all the lithium iron phosphate thin films were spin coated on the 3rd day of aging.

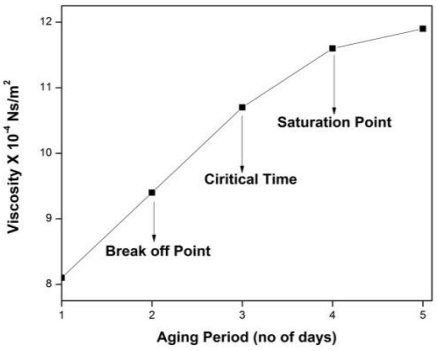

Fig.1 Effect of solute concentration on the viscosity of sol solution with respect to aging period (Li:Fe:P = 1:1:1)

3.2Thickness Measurement

The simplest method for thin film thickness determination is measuring mass gain of a coated substrate with a sensitive balance. Thickness'd' of coated thin film can be calculated from mass 'm' and density 'ρ' of the material deposited, and area 'A' on which the material is deposited. They can be related as

$$d = m/A\rho \tag{4}$$

By this method the film thickness can be determined with sufficient accuracy. The determined values of thickness were also verified with Mass profilometer. Thickness of $LiFePO_4$ thin films coated with 4 to 12 layers is given in Fig 2. It is understood that each coating layer makes an increment in the film thickness obviously.

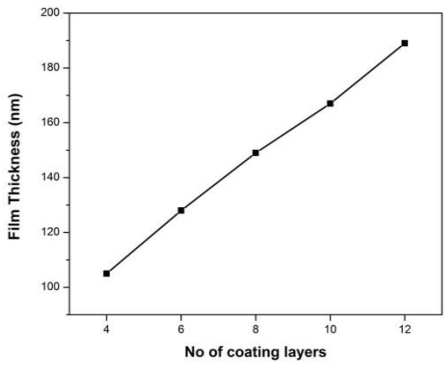

Fig.2 Variation of film thickness with different number of layer of $LiFePO_4$ thin films

3.3 Structural Characterization

As the thickness and morphological properties of the film varies with the number of coating cycles and thickness, the optimum number of coating cycles is to be optimized so as to get uniform coating as well as required thickness.

Uniform coating with required thickness can result in good surface morphological, structural and optical properties.

X ray diffraction patternof $LiFePO_4$ thin films coated with different number of coating layers 4 to 12 are shown in Fig 3. The diffraction peaks of all the samples have been identified as olivine structure, orthorhombic space group (Pnma) with preferred orientation along the (311) plane, the other orientations observed in the XRD profiles correspond to (200), (301), (212), (103) and (141) plane which is in well agreement with the standard JCPDS PDF data file number 83-2092. Sharpness and intensity of all peaks increasewith increase in number of coatings. This may be attributed to the increase in degree of crystallinity and densification of crystallite aggregates with number of coating cycles [28,29].The mean grain size (D) of $LiFePO_4$ thin films deposited with different number of coating layers have been calculated using the Scherrer's relation

$$D = 0.89\lambda / \beta \cos\theta \tag{5}$$

Where β is the full width at half maximum, λ is the wavelength of the incident X-ray and θ is the Bragg's diffraction angle. The mean grain size evaluated from the XRD data lie between 29.5 nm to 31.6 nm. The grain size increases with increase of number of coating layers and favors the growth parallel to the substrate surface.

It is found that while crystallization enhanced, the grain size also increased. The 12 cycles of coating resulted increase in thickness, grain size and volume of the films, making the film as nearly stress free.

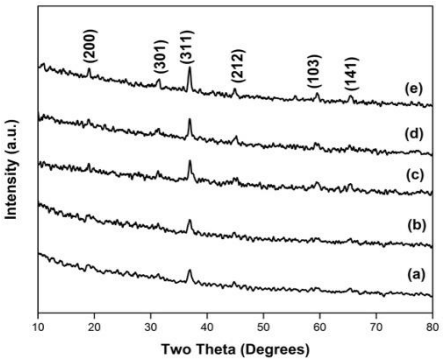

Fig 3. XRD pattern for $LiFePO_4$ thin films deposited with different number of coating layers(a) 4^{th} coat (b) 6^{th} coat (c) 8^{th} coat (d) 10^{th} coat and (e) 12^{th} coat

Micro strain (ε) of the crystallites varies inversely with mean grain size, and has been evaluated using the relation (6).

$$\varepsilon = \beta \cos\theta / 4 \tag{6}$$

Dislocation density (δ) defined as the length of dislocation per unit volume gives the amount of defects in a crystal and can be estimated using the relation (7).

$$\delta = 1/D^2 \tag{7}$$

A gradual decrease in micro strain and dislocation density of the crystallites with coating cycles is given in the table (1). This attributes the increase in the packing of crystallites with

number of coatings, causing increased thermal and mechanical shock resistance to the film surface. Preferred orientation of crystallites in $LiFePO_4$ thin film have been studied from the texture coefficient (TC) and calculated using the relation (8).

$$TC(hkl) = \frac{I_i(hkl)/I_0(hkl)}{1/N\sum^{N}_{i=1} I_i(hkl)/I_0(hkl)} \quad (8)$$

Where TC (hkl) is the texture coefficient of (hkl) plane, I_i(hkl) is measured intensity, I_0(hkl) is the standard intensity of JCPDS power diffraction pattern of corresponding peak [18]. The calculated texture coefficient is found to be maximum for the (311) plane indicating it as the preferred orientation. Further, the increase in TC (311) value with the different layer of the $LiFePO_4$ signify, the gradual increase in the oriented overgrowth of the crystallites along this plane, as evidenced in the XRD profile [30]. Also, to explain the growth mechanism the standard deviation σ was calculated by using the expression (9).

$$\sigma = \{(\Sigma I_{hkl}^2 - (\Sigma I_{hkl}^2/N))/N\}^{1/2} \quad (9)$$

Where 'I' denotes relative intensity of (hkl) plane. N is the number of reflections considered for the analysis. The standard deviation (σ) value is found to increase with the increase in film thickness indicating the excessive crystallite growth along the preferred (311) direction. The crystallographic parameters viz., mean grain size, micro strain, dislocation density, Texture coefficient and standard deviation of $LiFePO_4$thin films spin coated with different layers of coating have been evaluated from the XRD data and is shown in the Table 1

Table. 1 Various crystalline parameters evaluated from the XRD data of the $LiFePO_4$ thin films at different layers of coatings

.

Number of coatings	Grain Size (nm)	Micro Strain X 10^{15} (lines/$m^{2)}$)	Dislocation Density X 10^{-3} (lines.m^{-4})	Plane	Texture Coefficient	Standard Deviation
4	29.5	2.16	5.8155	(311) (301) (200)	1.0249 1.2490 1.5072	0.3865
6	30.0	2.14	5.7651	(311) (301) (200)	1.0590 1.2122 1.4402	0.3972
8	30.5	2.12	5.7248	(311) (301) (200)	1.0818 1.1755 1.3732	0.4110
10	31.2	2.09	5.6493	(311) (301) (200)	1.1063 1.1385 1.2057	0.4208
12	31.6	2.08	5.6191	(311) (301) (200)	1.1274 1.1387 1.1053	0.4327

For orthorhombic crystalslattice constants 'a', 'b' and 'c' are evaluated using the following relation (10)

$$1/d^2 = (h^2/a^2 + k^2/b^2 + l^2/c^2) \quad (10)$$

Where 'd' is the line spacing, 'a', 'b' and 'c' are the lattice parameter, (h k l) are Miller indices. The peak profile analysis and lattice parameter determination were carried out using JCPDS data.

The evaluated lattice parameter a=10.33 A^o, b=6.010 A^o and c= 4.693 A^o for the films deposited with 12 layers are in good agreement with the JCPDS data. The (311) preferred orientation is known to be more useful for lithium ions to intercalate and de-intercalate from the olivine $LiFePO_4$ structure [27].

3.4 Fourier Infrared Spectroscopy (FTIR) Analysis

Fourier transformed infrared (FTIR) spectrum for the film of 12 layers is shown in Fig 4. Apart from Li ions, FeO_6 and PO_4 ions are also form the framework of $LiFePO_4$ structure. As shown in the figure the regions of wave numbers (400-600 cm^{-1}) and 2100 cm^{-1} involves bending and stretching vibrations of $LiFePO_4$ thin film samples.

Bands at 2550 cm^{-1} corresponds to the active symmetric and asymmetric bending modes of P-O bonds. In the high wave number region, band observed at 3000 cm^{-1} is assigned to the antisymmetric stretching mode [31]. A big peak at 3750 – 3890 cm^{-1} observed in the spectrum corresponds to O-H group due to $FePO_4.2H_2O$. Bending and stretching modes of phosphate ions in $LiFePO_4$ are observed as listed in the table (Fig. 4). This spectrum evident that the sample is well crystallized $LiFePO_4$ [25,32].

1: 495 cm^{-1}	2: 2100 cm^{-1}	3: 2550 cm^{-1}	4: 3000 cm^{-1}
5: 3600 cm^{-1}	6: 3750 cm^{-1}	7: 3850 cm^{-1}	8: 3890 cm^{-1}

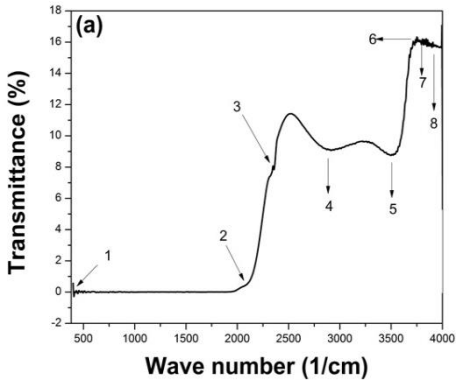

Fig 4. The FTIR images of $LiFePO_4$ thin filmdeposited with 12 layers of coating.

3.5 Morphological Analysis

Scanning electron micrographs of $LiFePO_4$ thin films deposited with 12 cycles of coating are shown in Fig 5. It shows 2 µm and 5 µm images displaying rough surface with spherical grains of various sizes. The bigger grains are the agglomeration of smaller grains. I shows porous nature of $LiFePO_4$ thin films deposited by the spin coating technique.

This void free, fully covered film morphology could be obtained by controlling deposition conditions such as number of coatings, spin rate, spin time, heat treatment temperature, solute concentration and annealing temperature. As shown in Fig. 5 the thickness of the prepared film is compact and adhered well to the substrate [20]. The average grain size and thickness are is about 200 nm and 1.8 µm, respectively for 12 cycles coated films. These spin coated films exhibited a narrow grain size distribution and small particles, agreed with the result of XRD patterns [2, 27].

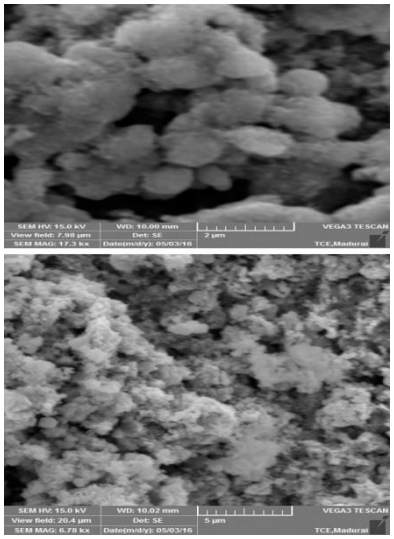

Fig 5. The SEM images of $LiFePO_4$ thin films deposited with 12 layers of coating

3.6 Optical Characterization

Wavelength dependent optical transmittance spectra of prepared $LiFePO_4$ thin films are shown in Fig 6(I) for 8, 10 and 12 cycles of coating. As can be seen, the thin films are highly transparent in the whole wavelength range from 300 nm to 1000 nm. The transmittance of the film is between 87.25 % and 90.75% for the whole spectral region. This observation reveals that the films are low absorptive[11]. Optical band gap of the prepared $LiFePO_4$ thin films were evaluated from their UV – vis transmittance spectra and absorption coefficient.
coefficient (α) was calculated from the transmittance spectra using the relation (11)[34]

$$\alpha = 4\pi k_f/\lambda \tag{11}$$

wherek_f is the extinction coefficient calculated from the experimental measurements using the relation

$$k_f = 2.303\lambda \log(1/T_o)/4\pi t \tag{12}$$

Where T_o is the transmittance, t is the thickness and λ is the wavelength of the incident radiation.
The optical band gap of the films was obtained theTauc relation (13) [35]

$$\alpha h\upsilon = A\,(h\upsilon - E_g)^{1/2} \tag{13}$$

Where 'α' is the optical absorption coefficient near the fundamental absorption edge, hυ is the photon energy.

The optical absorbance coefficient $(\alpha h\upsilon)^2$ as a function of photon of energy (hυ) for $LiFePO_4$ thin films are shown in Fig. 6(II). The variation of the optical absorption near the fundamental edge allows determining the energy band gap of $LiFePO_4$ thin films. Thus by extrapolating the linear part of the Tauc plot $(\alpha h\upsilon)^2$ vs. hυ (Fig. 6(II) a,b and c) on the energy axis gives the band gap value of 3.4 eV, 3.35 eV and 3 eV respectively [37].

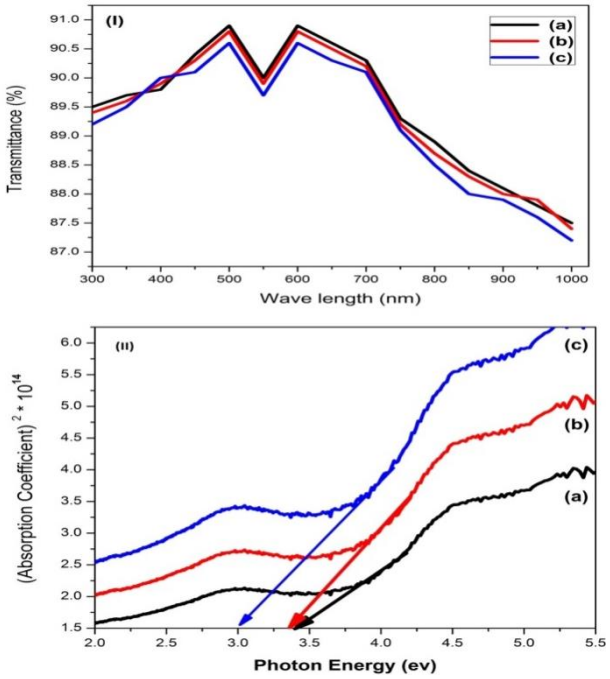

Fig 6. Optical studies for $LiFePO_4$ thin films (I) Optical Transmission spectra (II) Plots of $(\alpha h\upsilon)^2$ vs photon of energy ($h\upsilon$)

4. Conclusions

$LiFePO_4$ thin films were successfully fabricated onto glass substrates by the combination of sol-gel process and spin coating deposition using the optimized coating conditions. Optical, structural and morphological properties were studied. X- ray diffraction of8 - 12 layers of coating was identified as olivine structure, orthorhombic space group (Pnma) with preferred orientation along the (311) plane. The observed FTIR spectrum was assigned to stretching and bending modes of the phosphate group. Results of SEM observation showed dense and uniform growth of grains at higher coating cycles.

Thickness of the film was found to increase with the number of coating cycles. The grown films were highly transparent confirming the high quality films. The band gap energy of the films was found to be 3.4 eV from the Tauc plot of $(\alpha h\upsilon)^2$ vs photon of energy ($h\upsilon$).These observations and results are very encouraging since a costless and simple spin coating method can be used to prepare such films and open the way of possible valorization of the prepared films in many other applications.

References

[1] Susumu Shiraki, Yoshitaka Takagi, Ryota Shimizu, Tohru Suzuki, Masakazu Haruta, Yukio Sato, Yuichi Ikuhara, Taro Hitosugi, Thin solid Filims.**600,** 175 (2016).
[2] C. Julien., M.A. Camacho-Lopez., L.Escobar-Alarcon., E. Haro-Poniatowski., Materials Chemistry and Physics.**68,** 210 (2001).
[3] M.C. Rao, International Journal of Pure and Applied Physics**6**(3), 365 (2010).
[4]Susumu Shiraki, Hideki Oki, Yoshitaka Takagi, Tohru Suzuki, AkichikaKumatani, Ryota Shimizu, Masakazu Haruta, Takeo Ohsawa, Yukio Sato, Yuichi Ikuhara, Journal of Power Sources.,**267,** 881 (2014).
[5] Rong Huang., Taro Hitosugi, Craig A.J. Fisher, Yumi H. Ikuhara, Hiroki Moriwake, Hideki Oki, Yuichi Ikuhara, Materials Chemistry and Physics.**133,** 1101 (2012).
[6] Hui xia., Li lu., ElectrochimicaActa.**52,** 7014 (2007) .

[7]J.F. Whitacre, W.C. West, B.V. Ratnakumar, Journal of Power Sources.,**103,** 134 (2001) .
[8]J. Pracharova, J. Pridal, J. Bludska, I. Jakubec, V. Vorlicek, Z. Malkova, th.Dikonimos Makris, R. Giorgi, L. Jastrabik, Journal of Power Sources**108,** 204 (2002).
[9] Woo-Seong Kim, Journal of Power Sources **134**, 103 (2004).
[10] Woon-GiChoi., Soon-Gil Yoon, Journal of Power Sources.**125,** 236 (2004) .
[11] E. Rossen., J.N. Reimers, J.R. Dahn, Solid State Ionics.**62**, 53 (1993).
[12] Won-Sub Yoon., Sung-Ho Ban, Kyung-Keun Lee, Kwang-Bum Kim, Min Gyu Kim, Jay Min Lee, Journal of Power Sources. **97-98**, 282 (2001).
[13] Masahiko Hayashi., Masaya Takahashi, Yoji Sakurai, Journal of Power Sources. **174,** 990 (2007).
[14] Jin-Ho Lee.,Kyoo-Seung Han, Bum-Jae Lee, Seong-Il Seo, Masahiro Yoshimura, ElectrochimicaActa.**50,** 467 (2004).
[15] Ying Tao., Zhenhua Chen, Baojun Zhu, Weizhuang Huang, Solid State Ionics. **161,**187 (2003).
[16] Taeri Kwon., Tsuyoshi Ohnishi, KazutakaMitsuishi, Tadashi C. Ozawa, Kazunori Takada, Journal of Power Sources.**274**, 417 (2015).
[17] Guangfen Li., Jing Zhang, Applied Surface Science.,**258,** 7612 (2012).
[18] VaishaliPatil., Arun Patil, Ji-Won Choi, Seok-Jin Yoon, Solid State Sciences. **13,** 1232 (2011).
[19] H. Porthault., f. Le Cras, s. Franger, Journal of Power Sources.**195,** 6262 (2010).
[20] Chung-Ta Ni.,Kuan-Zong Fung, Solid State Ionics., **179**, 1230 (2008).
[21] F. Khatun, M.A. Gafur, M.S. Ali, M.S. Islam, M.A.R. Sark, Journal of Scientific Research **6**(2), 217 (2014).
[22] Mun-Kyu Kim, Kyu-Sung Park, Jong-Tae Son, Jin-Gyun Kim, Hoon-Taek Chung, Ho-Gi Kim, Solid State Ionics. **152-153,** 267 (2002).
[23] Ki Woong Kim., SeongIhl Woo, Kang-Hong Choi, Kyoo-Seung Han, Yong-Joon Park, Solid State Ionics.**159,** 25 (2003).
[24] L. Predoana, A. Barau, M. Zaharescu, H. Vassilchina, N. Velinova, B. Banov, A. Momchilov, Journal of European Ceramic Society **27,** 1137 (2007).
[25] K.J. Rao, H. Benqlilou-Moudden, B. Desbat, P.Vinatier, A. Levasseur, Journal of Solid State Chemistry **165**, 42 (2002) .
[26] M.C. Rao, S.K. Muntaz Begum, E. Sivanagi Reddy, M. Hussain, AIP Conf. Proc. **1447,** 613 (2012).
[27] H. PadmanabhaSarma., V. Subramanian., N. Rangarajan., K.R. Murali., Bulletin of Material Science **18,** 875 (1995).
[28] S. Tanemura., S. Miao., P. Jin., K. Kaneko., A. Terai., N. Nabatova- Gabain., Applied Surface Science.**654**, 654 (2003).
[29] P.J. Bouwman., B.A. Boukamp., H.J.M. Bouwmeester., C.V. Ramana., Solid State Ionics., **152,** 181(2002).
[30] K.V. Madhuri., K.S. Rao., B.S. Naidu., O.M. Hussain., Journal of Power Materials Science: Materials in Electronics.**13, 425** (2002).
[31] K. Kushida., K. Kuriyama., Solid State Communication.**118, 615**(2001) .
[32] J. Van Elp., J. Wieland., H. Eskes., P. Kuiper., G. A. Sawatzky., Physics Review. B. **44**, 6090 (1992) .
[33] T. Ohzuku., A. Ueda., Solid State Ionics.**69**, 201 (1994).
[34] H. PadmanabhaSarma., V. Subramanian., N. Rangarajan., K.R. Murali., Bulletin of Material Science **18,** 875 (1995).
[35] S. Tanemura., S. Miao., P. Jin., K. Kaneko., A. Terai., N. Nabatova- Gabain., Applied Surface Science.**654**, 654 (2003).
[36]P.J. Bouwman., B.A. Boukamp., H.J.M. Bouwmeester., C.V. Ramana., Solid State Ionics. **152,** 181(2002).
[37] VolkanSenay, SonerOzen, Suat Pat, SadanKorkmaz, The European Physical Journal D **69**, 76 (2015).